Molecular Therapy
Nucleic Acids
Original Article

MicroRNA-181d-5p-Containing Exosomes Derived from CAFs Promote EMT by Regulating CDX2/HOXA5 in Breast Cancer

Hongbin Wang,[1,3] Hong Wei,[2,3] Jingsong Wang,[1] Lin Li,[1] Anyue Chen,[1] and Zhigao Li[1]

[1]The Second Ward, Department of Breast Surgery, Harbin Medical University Cancer Hospital, Harbin 150081, People's Republic of China; [2]In-Patient Department of Ultrasound, The 2nd Affiliated Hospital of Harbin Medical University, Harbin 150001, People's Republic of China

Recently, novel mechanisms underlying the pro-tumorigenic effects of cancer-associated fibroblasts (CAFs) have been identified in several cancers, including breast cancer. CAFs can secrete exosomes that are loaded with proteins, lipids, and RNAs to affect tumor microenvironment. Herein, we identify CAF-derived exosomes that can transfer miR-181d-5p to enhance the aggressiveness of breast cancer. Cancerous tissues and matched paracancerous tissues were surgically resected from 122 patients with breast cancer. Chromatin immunoprecipitation (ChIP) and dual luciferase reporter assays were employed to identify interaction between homeobox A5 (HOXA5) and caudal-related homeobox 2 (CDX2), as well as between CDX2 and miR-181d-5p, respectively. Human breast cancer Michigan Cancer Foundation-7 (MCF-7) cells were cocultured with CAF-derived exosomes. 5-Ethynyl-2′-deoxyuridine (EdU) assay, TUNEL staining, Transwell invasion assays, and scratch tests were carried out to evaluate MCF-7 cell functions. Nude mice bearing xenografted MCF-7 cells were injected with CAF-derived exosomes, and the tumor formation was evaluated. HOXA5 expressed at a poor level in breast cancer tissues, and its overexpression retarded MCF-7 cell proliferation, invasion, migration, and epithelial-mesenchymal transition (EMT) and facilitated its apoptosis *in vitro*. miR-181d-5p targets CDX2, a transcription factor binding to HOXA5 promoter. Coculture of CAFs and MCF-7 cells showed that CAFs prolonged proliferation and antagonized apoptosis of MCF-7 cells via release of exosomes. Coculture of MCF-7 cells and exosomes derived from CAFs identified miR-181d-5p as a mediator of the exosomal effects on MCF-7 cells, in part, via downregulation of CDX2 and HOXA5. CAF-derived exosomes containing miR-181d-5p promoted the tumor growth of nude mice bearing xenografted MCF-7 cells. In conclusion, exosomal miR-181d-5p plays a key role in CAF-mediated effects on tumor environment in breast cancer, likely via CDX2 and HOXA5.

INTRODUCTION

Breast cancer is a frequently diagnosed female malignancy and one of the most common global cancer types.[1] Breast cancer therapy can be differentiated, according to histologic classifications, and metastatic breast cancer can be treated by hormone therapy if hormone receptors are expressed in tumor tissues.[2] However, breast cancer therapy is retarded by chronic iatrogenic effects of treatment on breast cancer survivors, such as infertility, constant pain, and fatigue.[3]

Cancer-associated fibroblasts (CAFs), which could regulate tumor metastasis by modulating extracellular matrix remodeling and growth factor signaling,[4] are critical elements of surrounding cancer stroma in the microenvironment of tumors. CAFs also own the ability to trigger epithelial-mesenchymal transition (EMT) in breast cancer cells.[5]

Exosomes, small membrane vesicles, ranging from 30 to 100 nm, are produced by many cells and can enter into the extracellular environment by binding to the plasma membrane.[6] Exosomal microRNAs (miRNAs) have been recognized as therapeutic targets and biomarkers of cancers.[7] Exosomal miRNA dysregulation in CAFs links to tumor invasion, metastasis, and poor prognosis.[8] For example, exosomal miRNAs released by CAFs can induce the EMT phenotype and stemness in various breast cancer cell lines.[9] miR-181 family members associate with the drug resistance, tumor formation, and metastasis in breast cancer.[10] Among them, miR-181d-5p correlates with the development of multiple tumors, such as osteosarcoma.[11] However, the detailed role of miR-181d-5p has not been thoroughly clarified in breast cancer.

Caudal-related homeobox 2 (CDX2) is a homeobox protein that associates with the differentiation of intestines in abnormal or normal locations.[12] CDX2 can be mediated by miR-181d in hepatic cells.[13] CDX2 polymorphism has been identified to be related with the susceptibility of breast cancer in Africans.[14] Therefore, we intended to explore the functional relationship of miR-181d-5p and CDX2 in breast cancer.

Predication based on JASPAR (http://jaspar.genereg.net/) suggested that there was a binding site between CDX2 and homeobox A5 (HOXA5). The HOX gene family contains a commonly seen

Received 23 September 2019; accepted 22 November 2019;
https://doi.org/10.1016/j.omtn.2019.11.024.

[3]These authors contributed equally to this work.

Correspondence: Zhigao Li, The Second Ward, Department of Breast Surgery, Harbin Medical University Cancer Hospital, No. 150, Haping Road, Nangang District, Harbin 150081, Heilongjiang Province, People's Republic of China.
E-mail: lzg_1964@yeah.net

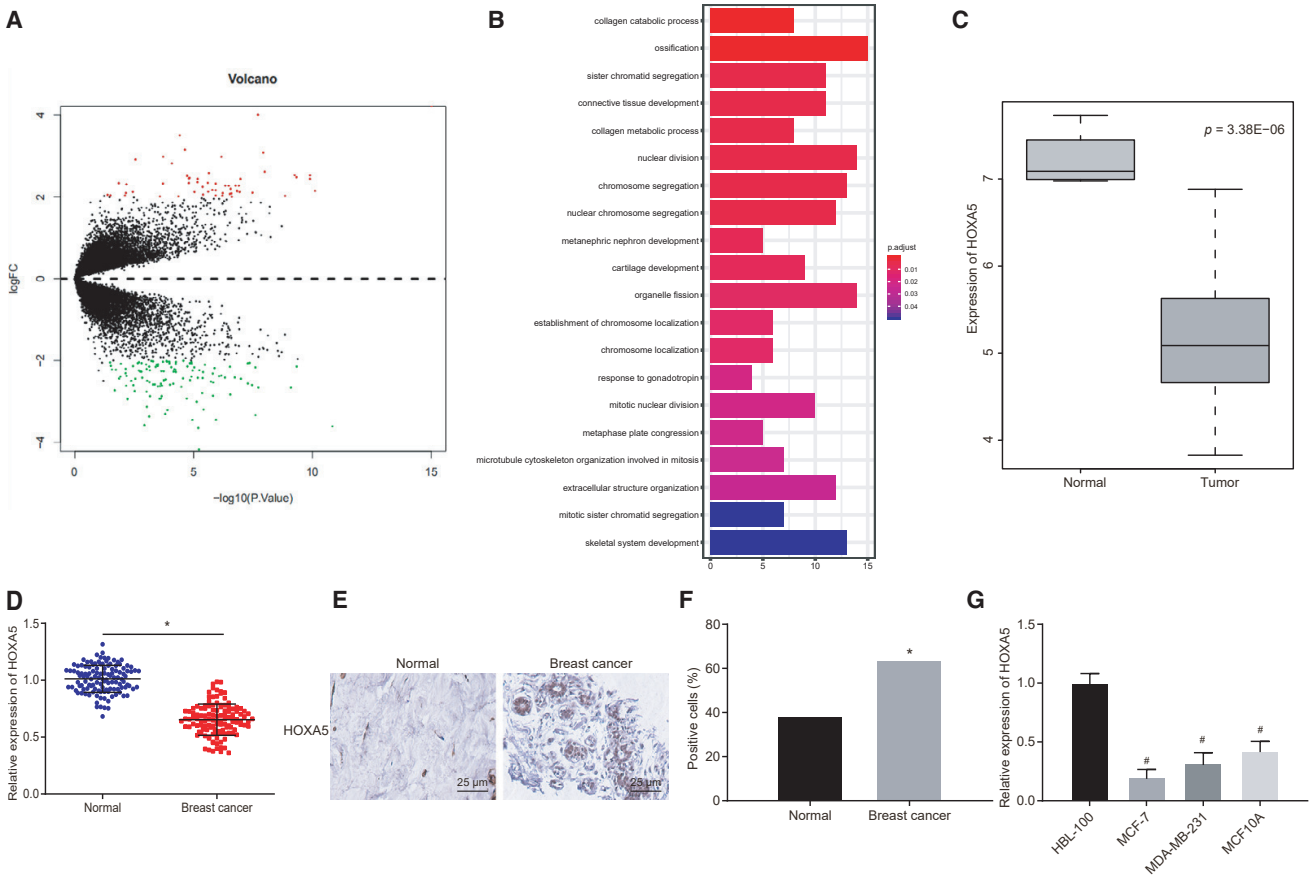

Figure 1. HOXA5 Is Expressed At a Poor Level in Breast Cancer Tissues and Cells

(A) Volcano map of differentially expressed genes in breast cancer. The abscissa represents log10 p value, and the ordinate represents logFC. Red dots represent upregulated genes in breast cancer, whereas green dots represent downregulated genes in breast cancer. (B) GO analysis for gene-enriched items of biological process. (C) Expression of HOXA5 in breast cancer tissues and adjacent normal tissues. (D) qRT-PCR analysis of HOXA5 expression in breast cancer tissues and adjacent normal tissues (n = 122). (E and F) Representative images (400 times) and quantitative analysis of HOXA5 expression in breast cancer tissues and adjacent normal tissues detected by immunohistochemistry (n = 122). (G) qRT-PCR analysis of HOXA5 expression in breast epithelial cell line HBL-100 and breast cancer cell lines (MCF-7, MDA-MB-231, and MCF10A). Data in (D) are measurement data and expressed as the mean ± SD, and comparisons between two groups are analyzed by paired t test. Data in (F) are enumeration data and expressed as number of cases or percentage. Comparisons between two groups are analyzed by chi-square test. Data in (G) are measurement data and expressed as the mean ± standard deviation, and comparisons among multiple groups are analyzed by ANOVA with Dunnett's post hoc test. The experiment is repeated three times. *p < 0.05 compared with adjacent normal tissues; #p < 0.05 compared with breast epithelial cell line HBL-100.

homeobox domain and plays a regulatory role as transcription factors.[15] Among them, the aberrant expression of HOXA5 has been found in cancers, indicating its role in tumor formation and progression.[16] More specifically, HOXA5 is intimately correlated with cell-fate transition and breast cancer progression.[17] Our study found that CAF-derived exosomal miR-181d-5p targeted CDX2 and HOXA5 to accelerate breast cancer progression, revealing its potential as a novel therapeutic target for breast cancer.

RESULTS

Low Expression of HOXA5 in Breast Cancer Tissues and Cells

Gene-expression datasets related to breast cancer GSE61304 and GSE59247 were retrieved from the Gene Expression Omnibus (GEO) database (https://www.ncbi.nlm.nih.gov/geo/) for differential analysis of gene expression. 57 upregulated genes and 119 downregulated genes were identified with log fold change (|logFC|) > 2 and a p value <0.05 as the screening threshold (Figure 1A). The "clusterProfiler" package was utilized for Gene Ontology (GO) analysis, which obtained gene-enriched items of biological process (Figure 1B). A previous study has demonstrated that the development of connective tissues (GO: 0061448) is of great predictive value for the prognosis of breast cancer.[18] Thus, genes involved in connective tissue development were chosen for the following study: the p value of the related target genes in GSE61304 was analyzed, and the gene with the lowest p value was selected as the key gene of breast cancer EMT (Table 1). Quantitative analysis on these three genes found that cartilage oligomeric matrix protein (COMP) and collagen type XI alpha 1 chain (COL11A1) were highly expressed, whereas HOXA5

Table 1. The Expression of COMP, COL11A1, and HOXA5 in Breast Cancer

	logFC	Average Expression	t	p Value	Adjusted p Value	B
COMP	3.08066	7.076846	6.552979	1.19E−08	1.03E−05	9.624154
COL11A1	4.004375	7.147385	6.425902	1.97E−08	1.30E−05	9.148658
HOXA5	−2.1021	5.315852	−5.09747	3.38E−06	0.000375	4.317088

COMP, cartilage oligomeric matrix protein; COL11A1, collagen type XI alpha 1 chain; HOXA5, homeobox A5.

was poorly expressed in breast cancer (Figure 1A). Meanwhile, differential analysis on GSE61304 identified the poor expression of HOXA5 in breast cancer (Figure 1C). Furthermore, qRT-PCR and western blot analysis elucidated that HOXA5 was expressed at a lower level in breast cancer tissues than that in adjacent normal tissues ($p < 0.05$) (Figure 1D). Immunohistochemistry found that HOXA5 was localized in cytoplasm and expressed poorly in breast cancer tissues ($p < 0.05$) (Figures 1E and 1F). Following that, qRT-PCR unraveled that compared with breast epithelial cell line HBL-100, poor expression of HOXA5 was detected in breast cancer cell lines (Michigan Cancer Foundation-7 [MCF-7], MDA-MB-231, and MCF10A), with the lowest expression found in MCF-7 ($p < 0.05$) (Figure 1G).

HOXA5 Overexpression Inhibits Proliferation, Invasion, Migration, and EMT and Induces Apoptosis of MCF-7 Cells

The expression of HOXA5 was altered in MCF-7 cells to investigate the effect of HOXA5 on proliferation, invasion, migration, EMT, and apoptosis of breast cancer cells. At first, qRT-PCR and western blot analysis revealed that cells transfected with the overexpressed HOXA5 (oe-HOXA5) plasmid exhibited higher HOXA5 expression, and those transfected with the short hairpin RNA targeting HOXA5 (sh-HOXA5) plasmid displayed lower HOXA5 expression (Figures 2A–2C). Next, the 5-ethynyl-2′-deoxyuridine (EdU) assay clarified that overexpression of HOXA5 decreased proliferative cells ($p < 0.05$) (Figure 2D). Then, TUNEL staining was employed to measure MCF-7 cell apoptosis, which revealed that overexpression of HOXA5 facilitated apoptosis of MCF-7 cells ($p < 0.05$) (Figure 2E). Transwell assay was used to assess MCF-7 cell invasion, which unraveled that HOXA5 overexpression repressed cell invasion ($p < 0.05$) (Figure 2F). Afterward, a scratch test on MCF-7 cell migration suggested that no statistical difference was found regarding relative migration distance of cells at 0 h ($p > 0.05$). After 48 h, overexpression of HOXA5 narrowed relative migration distance of MCF-7 cells, suggesting that cell migration ability was retarded ($p < 0.05$) (Figure 2G). It was shown by western blot analysis that transfection of the oe-HOXA5 plasmid enhanced expression of E-cadherin and vimentin and weakened expression of N-cadherin, Slug, Snail1, Twist1, ZEB1, and ZEB2 ($p < 0.05$) (Figures 2H and 2I). Hence, HOXA5 overexpression could promote apoptosis and inhibit proliferation, invasion, migration, and EMT of breast cancer cells.

Transcription Factor CDX2 Binds with the HOXA5 Promoter and Promotes Expression of HOXA5

The transcription factors that might bind to HOXA5 were predicted based on JASPAR (http://jaspar.genereg.net/), which revealed that transcription factor CDX2 might bind with promoter of HOXA5 (Figure 3A). Chromatin immunoprecipitation (ChIP) was performed to verify whether CDX2 could combine with the promoter of HOXA5, which revealed that the CDX2 antibody increased the enrichment of the HOXA5 promoter when compared with immunoglobulin G (IgG) (Figure 3C). qRT-PCR and western blot analysis identified lower CDX2 expression in breast cancer tissues (Figure 3B). Then, CDX2 was overexpressed or silenced in MCF-7 cells. qRT-PCR and western blot analysis displayed that HOXA5 expression was elevated by overexpressing CDX2 and decreased by silencing CDX2 (Figures 3D and 3E) ($p < 0.05$). Thus, HOXA5 expression was regulated by transcription factor CDX2. Downregulation of CDX2 inhibited HOXA5 expression, and upregulation of CDX2 promoted HOXA5 expression.

miR-181d-5p Targeted CDX2

To investigate further how CDX2 was regulated in breast cancer cells, differential analysis was conducted on breast cancer-related gene-expression dataset GSE59247, which screened out 46 upregulated miRNAs and 92 downregulated miRNAs. The first 50 miRNAs with the lowest p value were selected to plot the heatmap of differentially expressed miRNAs (Figure 4A). The miRNAs that targeted CDX2 were predicted based on TargetScan (http://www.targetscan.org/vert_72/), which predicted that miR-181d-5p could target CDX2 (Figure 4B). miR-181d-5p was also one of the differentially expressed miRNAs in GSE59247, and a previous study has reported that miR-181d-5p was involved in the occurrence of breast cancer,[10] suggesting that miR-181d-5p might regulate CDX2 in breast cancer.

The binding site of miR-181d-5p on CDX2 was identified, according to TargetScan (Figures 4A and 4B). Based on the results from the dual luciferase reporter assay, in the presence of the miR-181d-5p mimic, the luciferase activity of CDX2-wild type (WT) was decreased ($p < 0.05$), whereas that of CDX2-mutant (MUT) did not change ($p > 0.05$) (Figure 4D). Besides, the expression of miR-181d-5p was increased in breast cancer tissues (Figure 4C). After the expression of miR-181d-5p interfered in MCF-7 cells, qRT-PCR and western blot analysis were employed to determine CDX2 expression. It was demonstrated that the miR-181d-5p mimic decreased CDX2 expression, whereas the miR-181d-5p inhibitor elevated CDX2 expression ($p < 0.05$) (Figures 4E–4G). The above findings further proved that the expression of CDX2 was regulated by miR-181d-5p.

CAF-Derived Exosomes Prolonged Proliferation and Antagonized Apoptosis of MCF-7 Cells

To probe the effect of miR-181d-5p on breast cancer, fluorescent *in situ* hybridization targeting RNA (RNA-FISH) and immunofluorescence

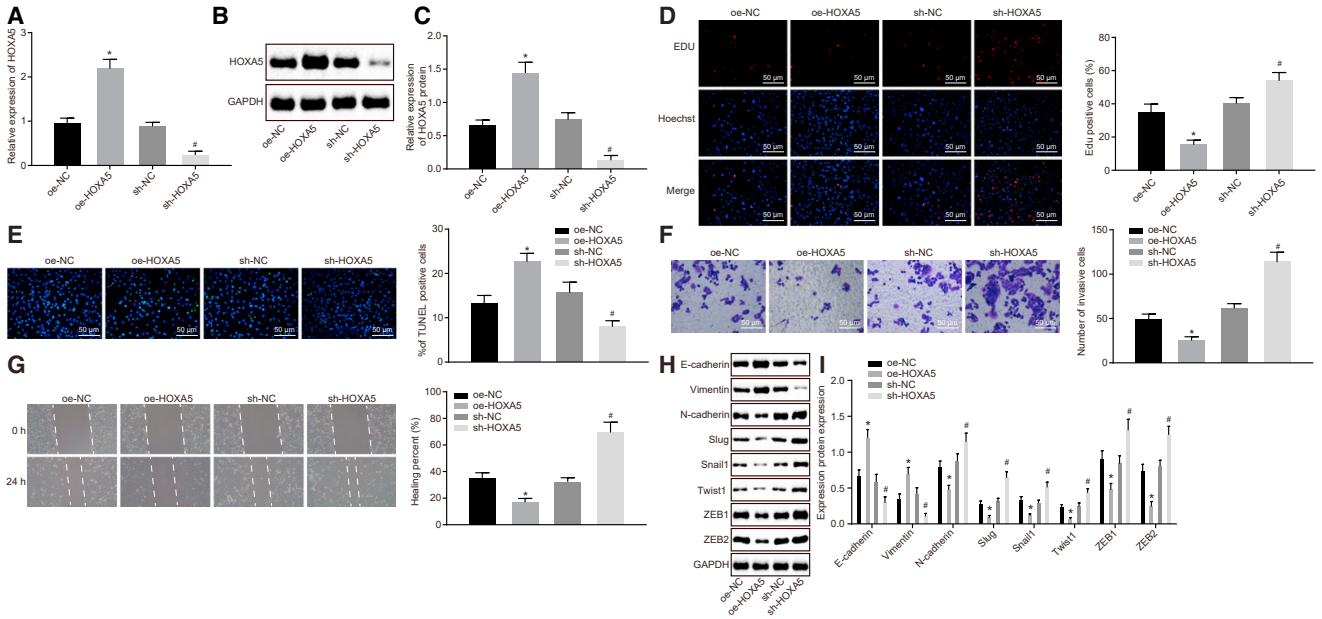

Figure 2. HOXA5 Overexpression Inhibits Proliferation, Invasion, Migration, and EMT and Induces Apoptosis of MCF-7 Cells

HOXA5 was overexpressed or silenced in MCF-7 cells. (A) qRT-PCR to assess HOXA5 expression in MCF-7 cells. (B and C) Western blot analysis of HOXA5 expression in MCF-7 cells. The band intensity is assessed. (D) EdU assay to detect MCF-7 cell proliferation (200 times). (E) TUNEL staining to analyze MCF-7 cell apoptosis (200 times). (F) Transwell assay to detect MCF-7 cell invasion (200 times). (G) Scratch test to detect MCF-7 cell migration (200 times). (H) Western blot analysis of expression of EMT-related proteins (E-cadherin, vimentin, N-cadherin, Slug, Snail1, Twist1, ZEB1, and ZEB2). (I) Statistical histograms of protein expression determined by western blot analysis. The band intensity is assessed. The above data are measurement data and expressed as the mean ± SD. Comparisons between two groups are analyzed by nonpaired t test. The experiment is repeated three times. *$p < 0.05$ compared with the treatment of oe-NC; #$p < 0.05$ compared with the treatment of sh-NC.

were utilized to determine miR-181d-5p expression in breast cancer cells (pan- cytokeratin [CK] positive) and tumor stroma (α-smooth muscle actin [SMA] positive). miR-181d-5p was highly expressed in both breast cancer cells and tumor stroma, with higher expression detected in tumor stroma (Figure 5A). CAFs and normal fibroblasts (NFs) were isolated from breast cancer tissues and adjacent normal tissues to detect the expression of fibroblast biomarkers. Relative to NFs, the expression of CAF-specific genes, including fibroblast activation protein (FAP); fibroblast-specific protein 1 (FSP1); actin alpha 2, smooth muscle (ACTA2); and CD90, was elevated in CAFs (Figure 5B). Immunofluorescence staining substantiated that both NFs and CAFs expressed vimentin, and only CAFs expressed α-SMA, the specific marker of CAFs (Figures 5C and 5D), suggesting the successful isolation of CAFs. It was then found that the expression of miR-181d-5p was higher in CAFs than in NFs (Figure 5F).

For the purpose of further studying the effect of CAFs on breast cancer, MCF-7 cells were treated with the culture medium (CM) of CAFs or NFs. EdU illustrated that CAF-CM promoted MCF-7 cell proliferation, whereas NF-CM exerted little effect on proliferation of MCF-7 cells (Figure 5G). Moreover, the retrieval of the EVmiRNA database (http://bioinfo.life.hust.edu.cn/EVmiRNA#!/browse) found that exosomes secreted from fibroblast contained miR-181d-5p (Figure 5E). Thus, it could be speculated that CAF-derived exosomes carrying miR-181d-5p could promote breast cancer progression. To verify this speculation, exosome inhibitor GW4869 was used to inhibit the production of exosomes from CAFs, and MCF-7 cells were treated with CAF-CM or NF-CM. EdU assay and TUNEL were performed to assess MCF-7 cell proliferation and apoptosis. Relative to NF-CM, cell proliferation was increased, and cell apoptosis was decreased after culture with CAF-CM, which was blocked by cotreatment of GW4869 (Figures 5H and 5I). Hence, CAF-derived exosomes could promote proliferation and inhibit apoptosis of breast cancer cells.

Exosomal miR-181d-5p Mediates Proliferation and Apoptosis of MCF-7 Cells, in Part, via Downregulation of CDX2 and HOXA5

To study the effect of exosomes derived from CAFs on breast cancer, exosomes were isolated from CAFs, which presented as uniform circle or oval membranous vesicles under a transmission electron microscope (TEM) (Figure 6A). The dynamic light scattering detected that the diameter of exosomes ranged from 30 nm to 120 nm (Figure 6B). Western blot analysis found that both CD63 and heat shock protein 70 (HSP70) were expressed at a higher level in exosome and its supernatant ($p < 0.05$) (Figure 6C). Flow cytometry found that the content of exosome surface marker CD63 was increased ($p < 0.05$) (Figure 6D). The studies above confirmed the successful isolation of exosomes. Then, PKH26 (red)-labeled exosomes were cocultured with MCF-7 cells for 48 h, and red fluorescence was observed in the surrounding area of MCF-7 cells under a confocal fluorescence

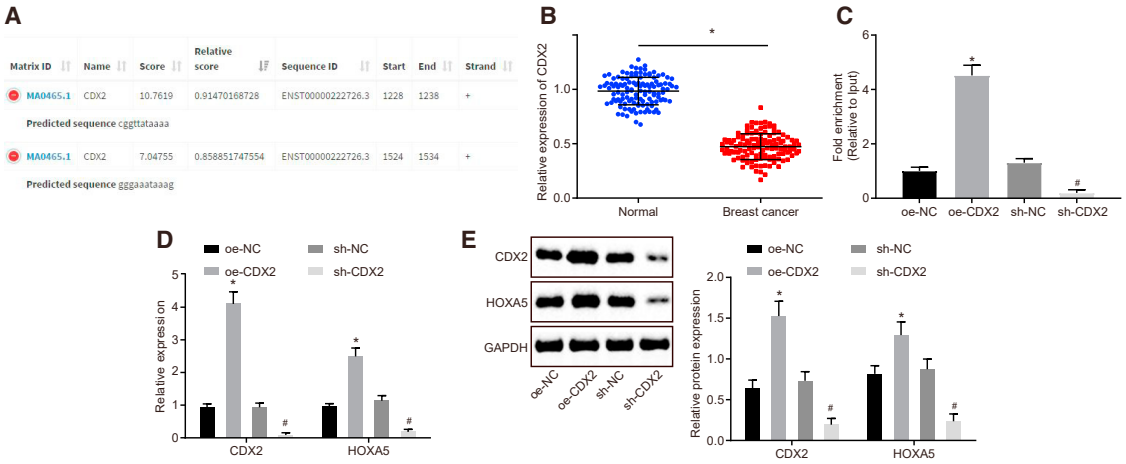

Figure 3. CDX2 Binds to the HOXA5 Promoter to Enhance Its Expression

(A) The binding region of CDX2 on the HOXA5 promoter predicted by JASPAR. (B) qRT-PCR analysis of CDX2 expression in breast cancer tissues and adjacent normal tissues (n = 122). (C) The interaction between CDX2 and HOXA5 verified by ChIP. (D) qRT-PCR analysis of CDX2 and HOXA5 expression in MCF-7 cells. (E) Western blot analysis of CDX2 and HOXA5 expression in MCF-7 cells. The above data are measurement data and expressed as the mean ± SD. Comparisons between two groups are analyzed by paired t test (B) and nonpaired t test (C–E). The experiment is repeated three times. *$p < 0.05$ compared with the treatment of oe-NC; #$p < 0.05$ compared with the treatment of sh-NC.

microscope, suggesting the absorption of CAF-derived exosomes by MCF-7 cells. Therefore, exosomes could transfer from donor cell CAFs to recipient cell MCF-7 cells (Figure 6E).

Afterward, MCF-7 cells were cocultured with exosomes. qRT-PCR and western blot analysis found out that the exo-miR-181d-5p mimic increased the expression of miR-181d-5p and decreased the expression of CDX2 and HOXA5, whereas the exo-miR-181d-5p inhibitor led to opposite trends (Figures 6F–6H), suggesting that CAF-derived exosomes carrying miR-181d-5p could transfer to breast cancer cells to regulate the expression of CDX2 and HOXA5. Following that, a series of *in vitro* experiments revealed that the exo-miR-181d-5p mimic increased proliferative cells, enhanced cell invasion and migration abilities, and repressed apoptosis of MCF-7 cells ($p < 0.05$), whereas the exo-miR-181d-5p inhibitor resulted in reverse tendency ($p < 0.05$) (Figures 6I–6L). Subsequently, western blot analysis unraveled that the exo-miR-181d-5p mimic led to reduced expression of E-cadherin and vimentin and elevated expression of N-cadherin, Slug, Snail1, Twist1, ZEB1, and ZEB2 in MCF-7 cells, whereas the exo-miR-181d-5p inhibitor induced opposite results ($p < 0.05$) (Figures 6M and 6N). Taken together, CAF-derived exosomes carrying miR-181d-5p could enhance proliferation, invasion, migration, and EMT and suppress apoptosis of breast cancer cells through regulation of CDX2 and HOXA5.

CAF-Derived Exosomes Containing miR-181d-5p Promote EMT in Breast Cancer by Regulating CDX2 and HOXA5 *In Vivo*

At last, to analyze the impact of CAF-derived exosomes on breast cancer growth and metastasis *in vivo*, nude mice were subcutaneously injected with MCF-7 cells to construct the xenograft tumor model. Then, the nude mice were treated with exosomes overexpressing or silencing miR-181d-5p by tail intravenous injection. Next, the tumor volume and weight of nude mice were measured. The injection of the exo-miR-181d-5p mimic led to faster tumor growth rate and increased tumor weight and volume ($p < 0.05$), whereas injection of the exo-miR-181d-5p inhibitor led to the opposite results ($p < 0.05$) (Figures 7A–7C). TUNEL staining was conducted to assess cell apoptosis in the xenograft tumor, which found that cell apoptosis was decreased by the injection of the exo-miR-181d-5p mimic and enhanced by injection of the exo-miR-181d-5p inhibitor (Figure 7D). The above results suggested that CAF-derived exosomes overexpressing miR-181d-5p promoted tumor growth and inhibited apoptosis of breast cancer.

Immunohistochemistry revealed that injection of the exo-miR-181d-5p inhibitor promoted expression of CDX2 and HOXA5 ($p < 0.05$) (Figure 7E). Afterward, western blot analysis revealed that the exo-miR-181d-5p mimic contributed to decreased expression of E-cadherin and vimentin and increased expression of N-cadherin, Slug, Snail1, Twist1, ZEB1, and ZEB2 in the xenograft tumor, which was reversed by the exo-miR-181d-5p inhibitor ($p < 0.05$) (Figures 7F and 7G). All in all, CAF-derived exosomes containing miR-181d-5p could facilitate EMT of breast cancer cells by regulating CDX2 and HOXA5.

DISCUSSION

Breast is the most intensively studied malignant tumor all over the world, owing to its high occurrence rate among women and the therapy of which remains to be a tough battle on many fronts.[19] CAFs accelerate breast cancer occurrence, growth, metastasis, and invasion.[20] The dysregulation of exosomal miRNAs plays a regulatory role in the initiation and activation of CAFs.[8] Collectively, our study

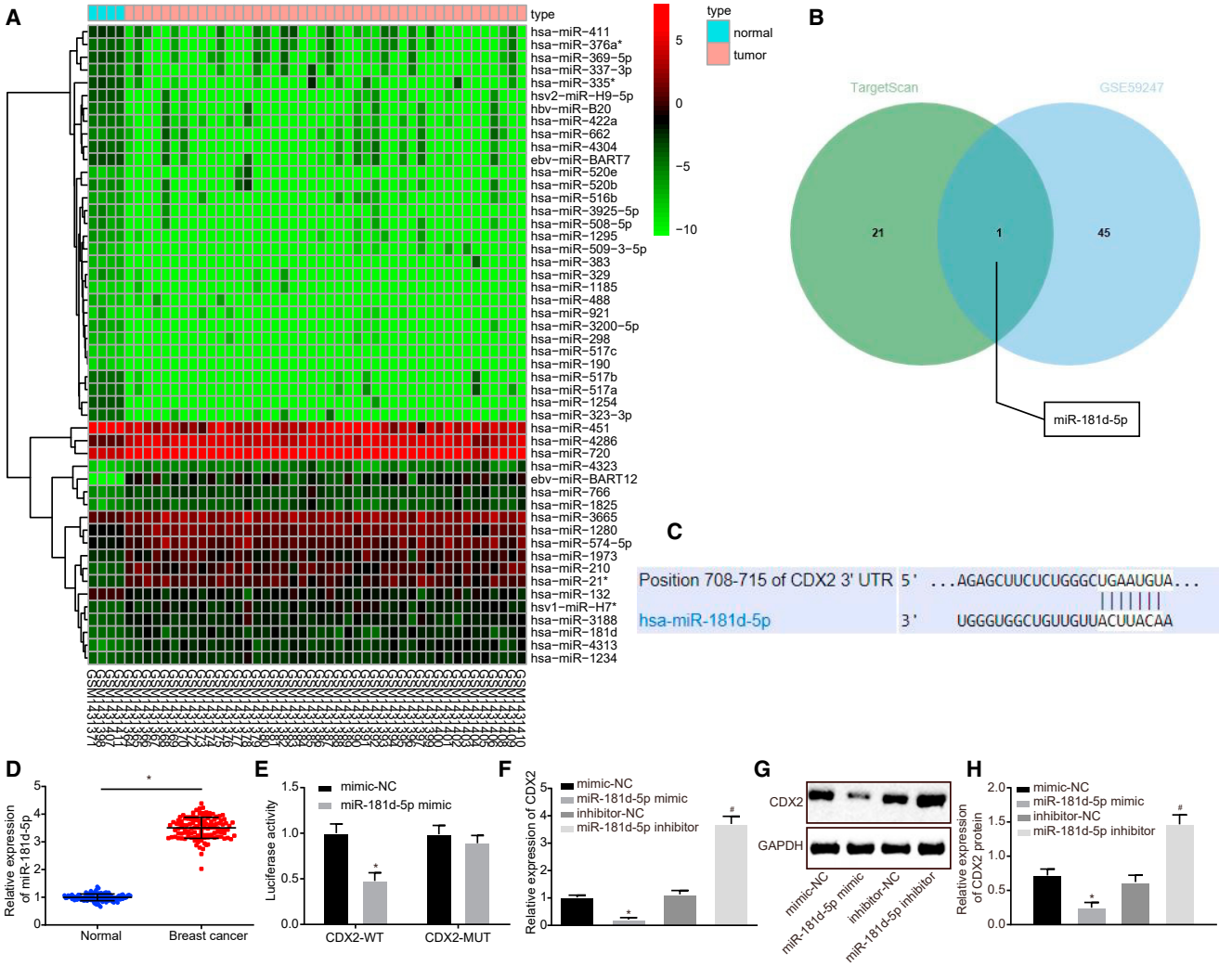

Figure 4. CDX2 Is the Target Gene of miR-181d-5p

(A) The predicted miRNAs that regulate CDX2. The blue part represents highly expressed miRNAs in breast cancer-related gene-expression dataset GSE59247, and the green part represents the predicted results from TargetScan. (B) The binding site of miR-181d-5p and CDX2 predicted by TargetScan. (C) qRT-PCR analysis of miR-181d-5p expression in breast cancer tissues and adjacent normal tissues (n = 122). (D) The target relationship between miR-181d-5p and CDX2 verified by dual luciferase reporter assay. (E) qRT-PCR analysis of CDX2 expression in MCF-7 cells. (F and G) Western blot analysis of CDX2 expression in MCF-7 cells. The band intensity is assessed. The above data are measurement data and expressed as the mean ± SD. Comparisons between two groups are analyzed by paired t test (C) and nonpaired t test (D, E, and G). (H) Statistical histograms of protein expression determined by western blot analysis. The experiment is repeated three times. *$p < 0.05$ compared with the treatment of mimic-NC; #$p < 0.05$ compared with the treatment of inhibitor-NC.

found out that CAF-derived exosomes carrying miR-181d-5p functioned as a promoter in EMT, proliferation, invasion, and migration and an inhibitor in apoptosis of breast cancer cells through CDX2 and HOXA5 reduction.

The initial finding of our study was that miR-181d-5p was highly expressed, whereas CDX2 and HOXA5 were poorly expressed in breast cancer. Consistent with this finding, miR-181d expresses at a high level in luminal breast cancer, which facilitates cell proliferation and cell entry at the S-phase.[10] The expression of miR-181a is higher in metastatic breast cancers, especially in triple-negative breast cancer.[21] Besides, the expression of CDX2 is downregulated in well and moderately differentiated tumors when compared with those poorly differentiated hepatocellular carcinomas.[22] CDX2 is also poorly expressed in colorectal cancer, causing gloomy progression-free survival.[23] Moreover, poor expression of HOXA5 has been detected in multiple breast cancer cell lines.[24] Relative to normal breast tissues, expression of HOXA5 is reduced in almost 70% of breast cancer tissues.[25] In addition, our study unraveled that CDX2 could promote HOXA5 expression by binding to its promoter region, and CDX2 was the target gene of miR-181d-5p. CDX protein was previously reported to interact with regulatory sequences of HOXA5, resulting in

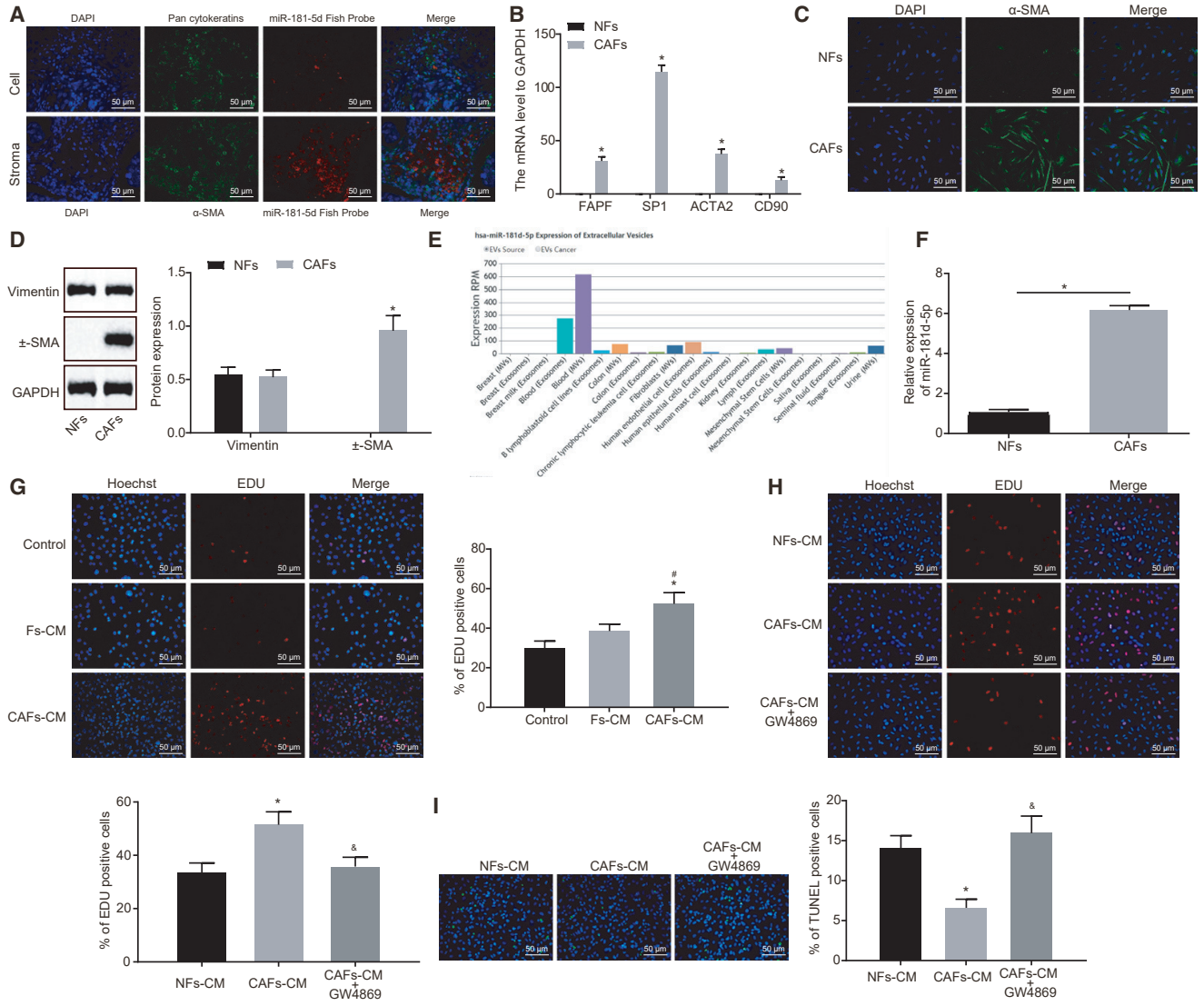

Figure 5. CAF-Secreted Exosomes Harboring miR-181d-5p Enhance Proliferation and Reduce Apoptosis of MCF-7 Cells

(A) The expression of miR-181d-5p in breast cancer cells and tumor stroma detected by RNA-FISH and immunofluorescence. (B) The expression of FAP, FSP1, ACTA2, and CD90 in CAFs and NFs. (C) Immunofluorescence of cellular morphology of NFs and CAFs. (D) western blot analysis of expression of vimentin and α-SMA in NFs and CAFs. The band intensity is assessed. (E) The expression of miR-181d-5p in exosomes secreted from fibroblast. (F) qRT-PCR analysis of miR-181d-5p expression in NFs and CAFs (n = 3). (G) EdU assay to detect MCF-7 cell proliferation (200 times). MCF-7 cells are treated with exosome inhibitor GW4869, CAF-CM, and NF-CM. (H) EdU assay to detect MCF-7 cell proliferation (200 times). (I) TUNEL staining to examine MCF-7 cell apoptosis (200 times). The above data are measurement data and expressed as the mean ± SD. Comparisons between two groups are analyzed by nonpaired t test. Comparisons among multiple groups are analyzed by ANOVA with Dunnett's post hoc test. The experiment is repeated three times. *p < 0.05 compared with NFs or NFs-CM; #p < 0.05 compared with the control group; &p < 0.05 compared with CAF-CM.

the regional expression of HOXA5 along the axial skeleton.[26] Meanwhile, a previous study has reported that CDX2 is modulated by miR-181d.[13]

Additionally, our study showed that HOXA5 overexpression elevated levels of E-cadherin and vimentin, whereas decreased levels of N-cadherin, Slug, Snail1, Twist1, ZEB1, and ZEB2, indicating that HOXA5 overexpression inhibited cell proliferation, invasion, migration, and EMT, whereas promoted cell apoptosis in breast cancer. E-cadherin, N-cadherin, vimentin, Snail, and Twist are known to be related to EMT with various expression levels between tumor tissues and adjacent normal tissues.[27] Interleukin 6 (IL-6) enhanced the EMT of MCF-7 cells, indicated by increased levels of vimentin, N-cadherin, Snail, and Twist, and decreased the E-cadherin level.[28] ZEB1 and ZEB2 are predominant EMT modulators that are positively associated with aggressiveness and EMT in breast cancer.[29] HOXA5 holds back

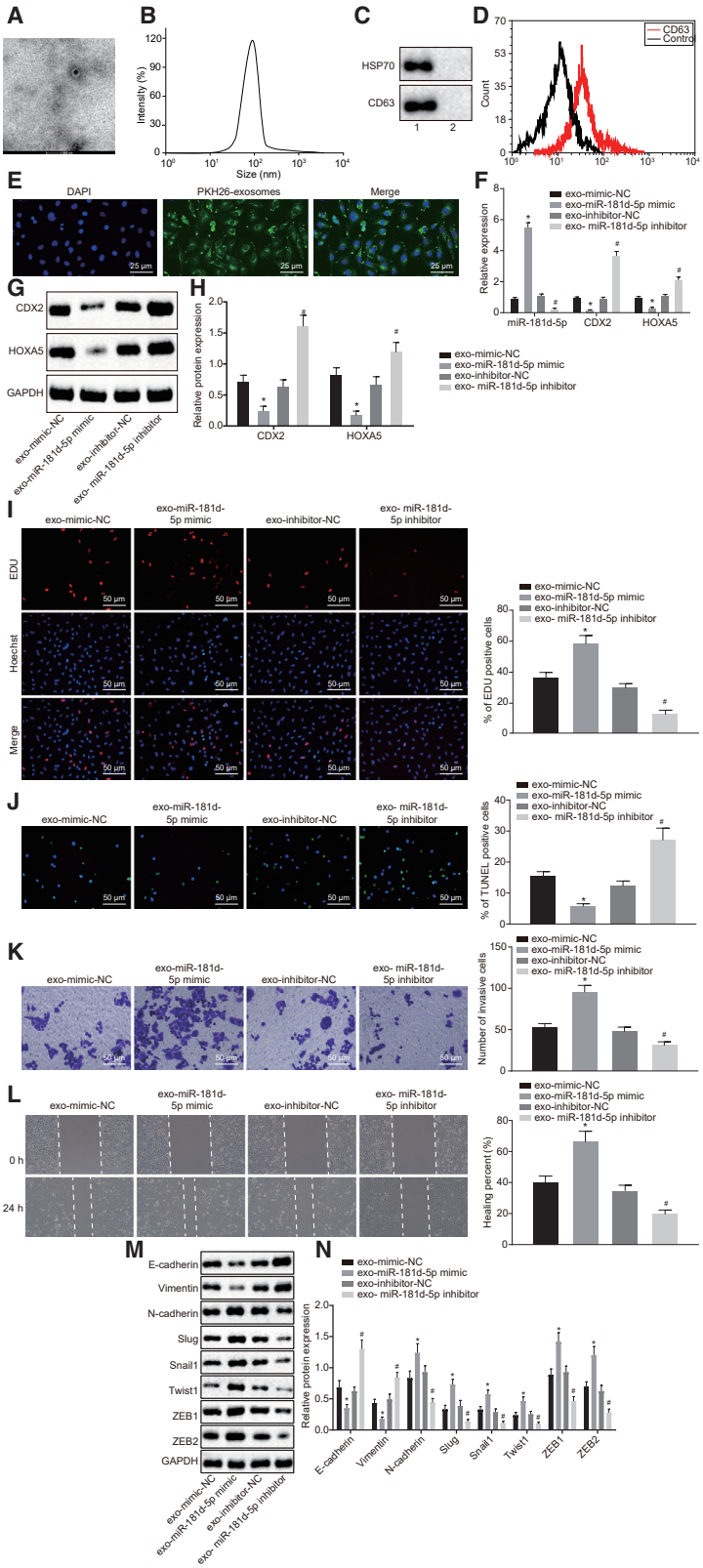

Figure 6. CAF-Secreted Exosomes Harboring miR-181d-5p Facilitate Proliferation, Invasion, Migration, and EMT and Inhibit Apoptosis of Breast Cancer Cells by Repressing CDX2 and HOXA5

(A) The identification of exosomes under a TEM (20,000 times). (B) The diameter of exosomes detected by the dynamic light scattering. (C) Western blot analysis of expression of exosome surface markers CD63 and HSP70. Lane 1, extractive exosomes; lane 2, the supernatant of exosomes. (D) Flow cytometry to detect the extent of exosome surface marker CD63. PKH26 (red)-labeled exosomes are cocultured with MCF-7 cells. (E) The uptake of exosomes by MCF-7 cells under an inverted microscope (400 times). (F) qRT-PCR analysis of the expression of miR-181d-5p, CDX2, and HOXA5 in MCF-7 cells. (G and H) Western blot analysis of the expression of CDX2 and HOXA5 in MCF-7 cells. The band intensity is assessed. (I) EdU assay of MCF-7 cell proliferation (200 times). (J) TUNEL staining of MCF-7 cell apoptosis (200 times). (K) Transwell assay of MCF-7 cell invasion (200 times). (L) Scratch test of MCF-7 cell migration (200 times). (M and N) Western blot analysis of the expression of E-cadherin and vimentin, N-cadherin, Slug, Snail1, Twist1, ZEB1, and ZEB2 in MCF-7 cells. The band intensity is assessed. The above data are measurement data and expressed as the mean ± SD. Comparisons between two groups are analyzed by nonpaired t test. The experiment is repeated three times. *$p < 0.05$ compared with exo-mimic-NC; #$p < 0.05$ compared with exo-inhibitor-NC.

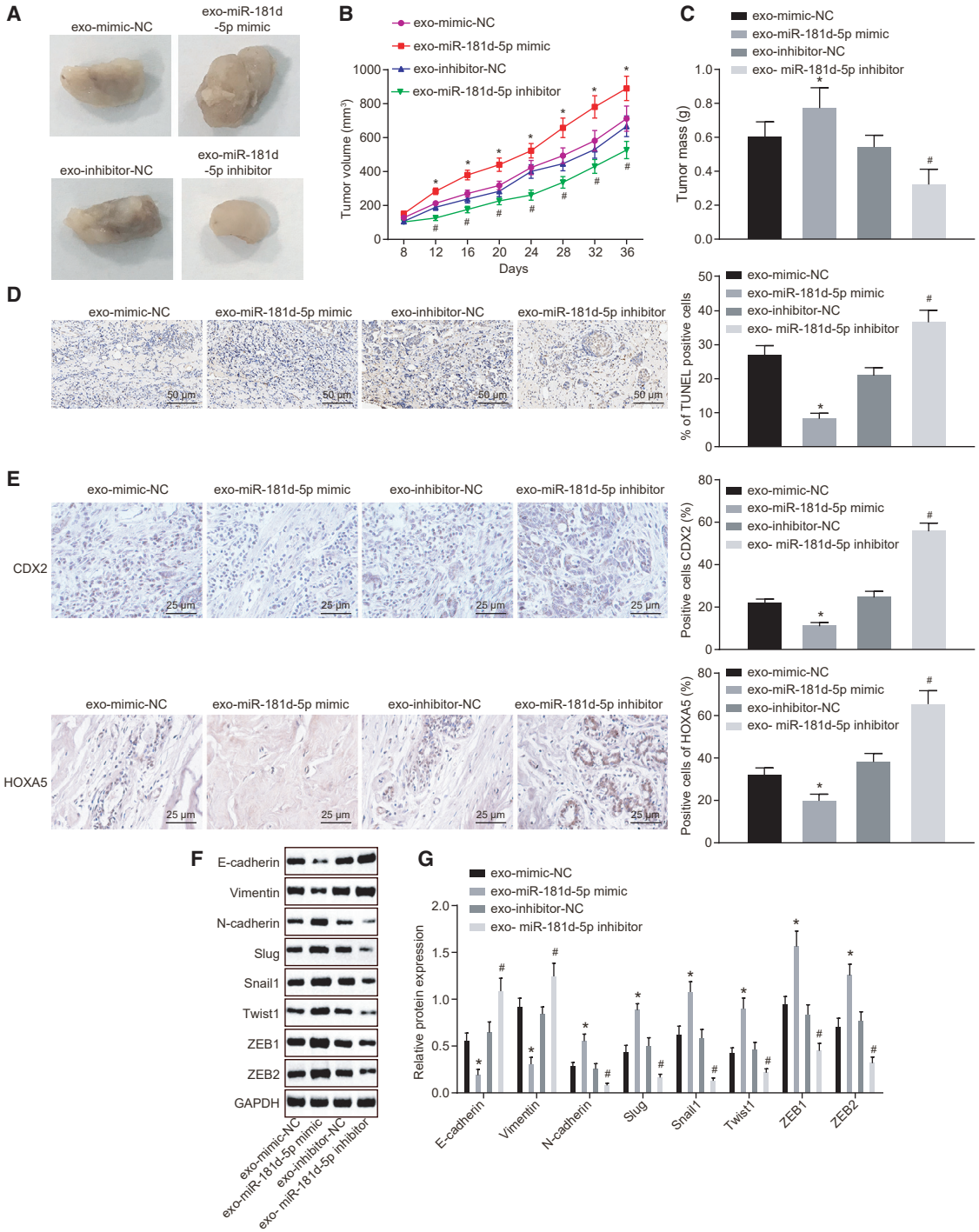

Figure 7. CAF-Secreted Exosomes Containing miR-181d-5p Accelerate EMT by Inhibiting CDX2 and HOXA5

The nude mice are treated with exo-miR-181d-5p mimic or exo-miR-181d-5p inhibitor by tail intravenous injection. (A) The morphology of xenograft tumor in nude mice (n = 6). (B) Tumor volume of xenograft tumor in nude mice (n = 6). (C) Tumor mass of xenograft tumor in nude mice (n = 6). (D) TUNEL staining of cell apoptosis in xenograft tumor of nude mice (200 times). (E) Immunohistochemistry of expression of CDX2 and HOXA5 (400 times). (F and G) Western blot analysis of the expression of E-cadherin, vimentin, N-cadherin, Slug, Snail1, Twist1, ZEB1, and ZEB2 in xenograft tumor of nude mice. The band intensity is assessed. The above data are measurement data and expressed as the mean ± SD. Comparisons between two groups are analyzed by nonpaired t test. Comparisons at various time points are analyzed by repeated-measurement ANOVA (B). The experiment is repeated three times. *$p < 0.05$ compared with the treatment of exo-mimic NC; #$p < 0.05$ compared with the treatment of exo-inhibitor NC.

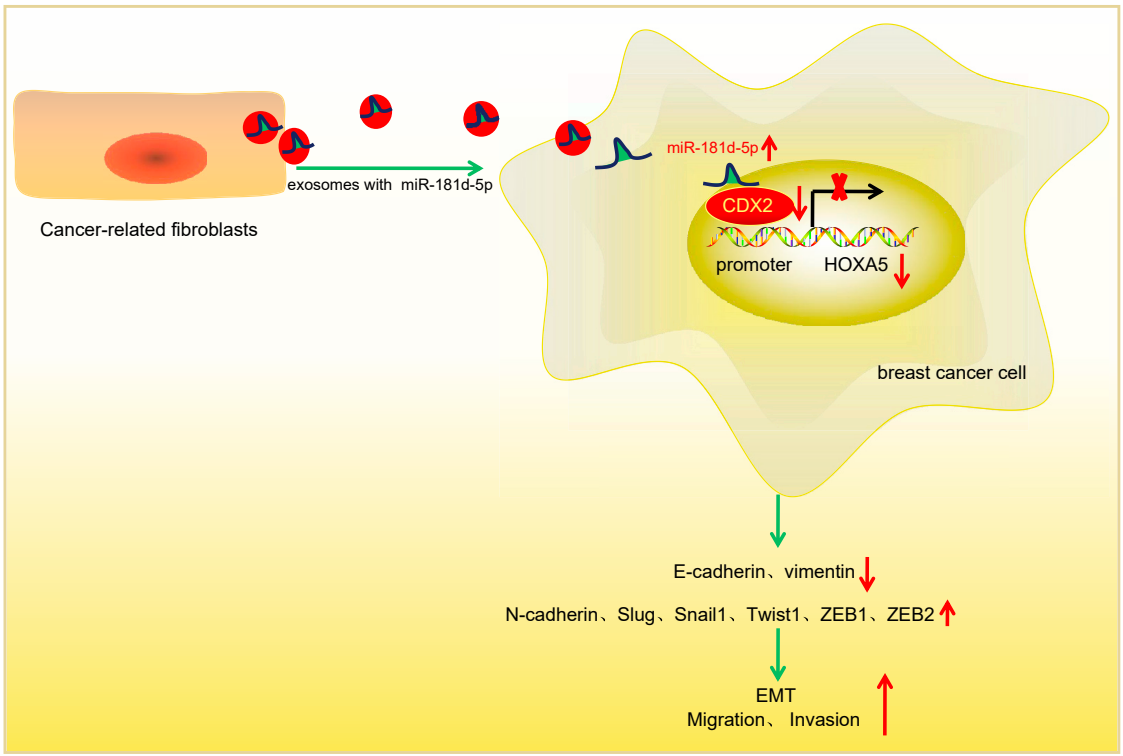

Figure 8. CAF-Secreted Exosomes Containing miR-181d-5p Promote EMT of Breast Cancer by Regulating CDX2 and HOXA5

Exosomes released from CAFs transfer miR-181d-5p into breast cancer cells and target transcription factor CDX2, which inhibits the binding of CDX2 to HOXA5 promoter region to repress HOXA5 expression, thus promoting EMT, migration, and invasion of breast cancer cells.

breast cancer initiation and progression by modulating CD24 and E-cadherin.[17] However, the absence of HOXA5 could cause promotion of breast cancer and abnormal regulation of the cell cycle through functional activation of Twist.[30] Chen et al.[31] have found that HOXA5 elevation contributes to breast cancer cell apoptosis. HOXA5 overexpression could repress cell invasion and migration *in vitro* and inhibit metastatic potential *in vivo* in highly invasive, non-small cell lung cancer cells.[15]

What is more, in our current work, we reveled that breast cancer MCF-7 cells could take in exosomes derived from CAFs, which contained miR-181d-5p. Exosomes, small membrane vesicles, can be collected from both normal and cancer cells.[32] Exosomal miRNA has been considered as an attractive biological marker for cancers.[33] For example, the conveyance of miR-9 mediated by exosomes could result in the induction of CAF-like properties in human breast fibroblasts.[34] Moreover, the most intriguing finding in our study showed that CAF-derived exosomes carrying miR-181d-5p induced EMT, cell proliferation, invasion, and migration, whereas impaired apoptosis in breast cancer by downregulating CDX2 and HOXA5. Dysregulation of exosomal miRNAs in CAFs is linked to tumor invasion, migration, and metastasis.[8] For example, the association between exosomal miR-373 and triple-negative and more aggressive breast cancers has been illustrated by Eichelser et al.[35] CAF-derived exosomal miRNAs contribute to the production of the EMT phenotype, as well as stemness in breast cancer.[9]

Taken together, CAF-secreted exosomal miR-181d-5p could facilitate a novel aspect of the treatment of breast cancer patients as result of its promotive effect on EMT, cell proliferation, invasion, and migration and inhibitory effect on apoptosis in breast cancer (Figure 8). Investigation of CAF-derived exosomes carrying miR-181d-5p yields a better understanding for therapy of breast cancer.

MATERIALS AND METHODS

Ethics Statement

Written, informed consent was obtained from all patients prior to the study. Study protocols were approved by the Ethic Committee of Harbin Medical University Cancer Hospital and based on the ethical principles for medical research involving human subjects of the Helsinki Declaration. The animal experiments were performed in strict accordance with the recommendations in the *Guide for the Care and Use of Laboratory Animals* of the National Institutes of Health. The protocol of animal experiments was approved by the Institutional Animal Care and Use Committee of Harbin Medical University Cancer Hospital. The animal experiments were conducted based on minimized animal number and the least pains on experimental animals.

Study Subjects

Breast cancer tissues and adjacent normal tissues were collected from 122 patients who were pathologically diagnosed as nonspecific invasive breast cancer and had received surgical resection in Harbin Medical University Cancer Hospital from April 2014 to August 2017. All patients had not received chemotherapy or radiotherapy or taken any hormonal drugs prior to the operation. There were 81 cases aged <50 years and 41 cases aged ≥50 years. According to World Health Organization (WHO) grading criteria,[36] 89 cases were diagnosed at grade I + II and 33 cases at grade III. Based on the sixth edition of the tumor node metastasis (TNM) staging criteria of the American Joint Committee on Cancer (AJCC),[37] 72 cases were diagnosed at stage I + II and 50 cases at stage III. Lymph node metastasis was not observed. One part of the specimens was fixed by 10% formaldehyde, dehydrated, embedded in paraffin, and sectioned into 4-μm slices. The remaining part was quickly frozen in liquid nitrogen and preserved at −80°C for RNA and protein extraction.

Immunohistochemistry

The paraffin sections of breast cancer tissues, adjacent normal tissues, and nude mice xenograft tumor specimens were de-waxed, dehydrated, and retrieved by water bath in antigen-retrieval liquid. Next, the sections were blocked with normal goat serum (C-0005; Shanghai Haoran Biological Technology, Shanghai, China) at room temperature for 20 min. Later, the sections were probed with primary antibody rabbit anti-CDX2 (ab88129, 1:100) and HOXA5 (ab82645, 1:100) at 4°C overnight and then with secondary antibody goat anti-rabbit IgG (ab6785, 1:1,000) at 37°C for 20 min. The above antibodies were purchased from Abcam (Cambridge, MA, USA). After that, the sections were reacted with horseradish peroxidase (HRP)-labeled streptomycin protein working solution (0343-10000U; Yi Mo Biological Technology, Beijing, China) at 37°C for 20 min, colored by diaminobenzidine (DAB) (ST033; Whiga Biosmart, Guangzhou, Guangdong, China), counterstained by hematoxylin (PT001; Shanghai Bogoo Biological Technology, Shanghai, China) for 1 min, blued by 1% ammonium hydroxide, sealed by neutral gum, observed, and photographed under a microscope. Finally, five random fields were selected from each section, and 100 cells were counted in each field. Positive cells <10% were regarded as negative, 10% ≤ positive cells <50% as positive, and positive cells >50% as strongly positive.[38]

TUNEL Staining

The sections were de-waxed, dehydrated, and incubated with 50 μL of 1% proteinase K diluent at 37°C for 30 min and with 0.3% H_2O_2 methanol solution at 37°C for 30 min to remove endogenous peroxidase activity. After the addition of TUNEL reaction liquid and 50 μL Converter-POD, the sections were incubated in a 37°C wet box away from light for 1 h and 30 min, respectively. Later, the sections were visualized by 2% DAB developing solution at room temperature for 15 min, and the reaction was terminated by distilled water. After that, the sections were counterstained by hematoxylin; dehydrated by 50%, 70%, 90%, and 100% ethanol; cleared by xylene; mounted by neutral gum; and observed under a 400-fold optical microscope. Ten random fields were selected from each section to count the number of positive cells. The ratio of apoptotic cell number to total cell number was viewed as the apoptotic index.

After fixed by 4% paraformaldehyde for 30 min, the cells were treated with 0.3% H_2O_2-formaldehyde solution (30% H_2O_2:formaldehyde = 1:99) for 30 min and 0.3% Triton X-100 on ice for 2 min. TUNEL reaction mixed liquor was prepared, according to the instructions of TUNEL cell apoptosis detection kit (green fluorescence; C1088; Beyotime Biotechnology, Shanghai, China). Cells were incubated with 50 μL terminal deoxynucleotidyl transferase (TdT) and 450 μL fluorescein-labeled 2′-deoxyuridine 5′-triphosphate (dUTP) solution at 37°C in the dark for 60 min, sealed with anti-fluorescence quenching mounting liquid, and observed under a fluorescence microscope. The excitation wavelength was 450 nm, and the emission wavelength was 550 nm (green fluorescence).

qRT-PCR

Total RNA was extracted from breast cancer and adjacent normal tissues or cells by using Trizol kit (15596-018; Beijing Solarbio Life Sciences, Beijing, China). Reverse transcription was conducted according to the instructions of cDNA reverse transcription kit (K1622; Beijing Ya'anda Biotechnology, Beijing, China). β-Actin was used as the internal control, and the relative transcription level of target genes was calculated by the $2^{-\Delta\Delta Ct}$ method.[39] All primers used in this study were synthesized by Takara Holdings (Kyoto, Japan) (Table 1).

Western Blot Analysis

Radioimmunoprecipitation assay (RIPA) cell lysis buffer (Beyotime Biotechnology, Shanghai, China) was used to extract breast cancer and adjacent normal tissues or cells. A bicinchoninic acid (BCA) kit (20201ES76; Yeasen Company, Shanghai, China) was utilized to determine protein concentration. After separated by PAGE, the protein was transferred onto the polyvinylidene fluoride (PVDF) membrane. Nonspecific binding was blocked by addition of 5% BSA at room temperature for 1 h. Subsequently, the protein was incubated with primary antibody rabbit anti-human CDX2 (ab88129, 1:2,000), HOXA5 (ab140636, 1:2,000), E-cadherin (ab15148, 1:500), vimentin (ab137321, 1:2,000), N-cadherin (ab18203, 1:100), Slug (ab106077, 1:2,000), Snail1 (ab82846, 1:300), Twist1 (ab50581, 1:2,000), zinc finger E-box-binding homeobox (ZEB)1 (ab124512, 1:3,000), ZEB2 (ab138222, 1:800), and glyceraldehyde-3-phosphate dehydrogenase (GAPDH) (ab8245, 1:5,000) at 4°C overnight. After rinsing with Tris-buffered saline with Tween-20 (TBST), three times (5 min each), the protein was incubated with HRP-labeled goat anti-rabbit IgG (ab205718, 1:20,000) at room temperature for 1 h and visualized by developing liquid. The protein quantitative analysis was conducted using ImageJ 1.48u software (National Institutes of Health, Bethesda, MD, USA) according to the gray value ratio of target band to that of GAPDH band.

Cell Treatment

Breast cancer epithelial cell lines (MCF-7, MDA-MB-231, and MDA-10A) and human normal breast epithelial cell line HBL-100 were

purchased from the cell bank of Typical Culture Preservation Committee of Chinese Academy of Science. The cells were incubated with DMEM, supplemented with 10% fetal bovine serum (FBS) and penicillin/ streptomycin (Gibco by Life Technologies, Grand Island, NY, USA) at 37°C with 5% CO_2.

Next, MCF-7 cells in the logarithmic growth phase were plated into a 6-well plate (4×10^5 cells/well). When cell confluence reached 70%–80%, the cells were transfected with mimic-negative control (NC), miR-181d-5p mimic, inhibitor-NC, miR-181d-5p inhibitor, oe-NC, oe-HOXA5, sh-NC, or sh-HOXA5, based on the manuals of Lipofectamine 2000 (11668-019; Invitrogen, New York, CA, USA). All of the plasmids were purchased from Shanghai GenePharma (Shanghai, China).

Isolation and Culture of CAFs

The tissue blocks of breast cancer were sectioned into the size of 1 mm^3 and detached with 0.1% collagenase III (Worthington Biochemical, Lakewood, NJ, USA) and 125 units/mL hyaluronidase at 37°C overnight. The undetached tissues were filtered, and the matrix cells were centrifuged at 178 × *g* for 5 min. The supernatant was resuspended by DMEM containing 10% FBS and cultured at 37°C with 5% CO_2. The isolation of NFs in adjacent normal tissues was performed similarly.

Extraction and Identification of CAF-Derived Exosomes

When cell confluence reached 80%–90%, CAFs were cultured with serum-free medium for 24 h. After cells were centrifuged at 2,000 × *g* at 4°C for 20 min, cell debris was removed, and the supernatant was centrifuged at 10,000 × *g* at 4°C for 1 h. The precipitation was suspended by serum-free DMEM containing 25 mM 4-(2-hydroxyethyl)-1-piperazineethanesulfonic acid (HEPES; pH 7.4) and underwent high-speed centrifugation again. After the supernatant was discarded, the precipitation was preserved at −80°C for later use.

30 μL exosomes were added on the copper grid and allowed to stand for 1 min. After that, exosomes were counterstained with 30 μL phosphotungstic acid solution (pH 6.8) at room temperature for 5 min. A TEM was used to observe exosomes following the manuals of the qNano kit (Izon Science, New Zealand).

Then, CAFs derived from exosomes were incubated by 1 mL PBS, supplemented with 1% BSA at room temperature for 30 min to block nonspecific antigen before centrifugation at 178 × *g* for 5 min. After that, the supernatant was discarded, and exosomes were resuspended by PBS. Exosomes were probed with CD63-phycoerythrin (PE) antibody at room temperature for 30 min, centrifuged at 178 × *g* for 5 min, and resuspended by 1% BSA-containing PBS. Afterward, exosomes were loaded and detected by a flow cytometer (Guava easyCyte system). qRT-PCR was performed to determine miR-181d-5p expression in exosomes.

Coculture of CAF-Derived Exosomes and Breast Cancer Cells

CAFs were treated with exosome inhibitor GW4869 to inhibit the release of exosomes. CAFs were cultured in the 6-well plate at the density of 1×10^6 cells/well. When cell confluence reached 80%–90%, cells were treated with 10% GW4869 (D1692-5MG; Sigma-Aldrich, St. Louis, MO, USA). After 24 h, cells and the supernatant were collected for later use.

CAF-derived exosomes were labeled, according to the instructions of PKH26 (red) dye liquid (MINI67-1KT; Sigma-Aldrich, St. Louis MO, USA) and then cocultured with breast cancer cells, which were inoculated into a 24-well plate for 48 h.

EdU Staining

MCF-7 cells were plated into a 96-well plate at the density of 5×10^3 cells/well. After 6 h, the cells were incubated with EdU medium (100 μL/well) for 2 h and fixed with cell stationary liquid, supplemented with 4% paraformaldehyde (100 μL/well) at room temperature for 30 min. The cells were incubated with glycine (2 mg/mL) for 5 min, 100 μL/well penetrant (PBS supplemented with 0.5% Triton X-100) for 10 min, and 1 times Apollo dye reaction liquid (100 μL/well) in the dark for 30 min. After rinsing with 100 μL/well penetrant, three times (10 min each), and 100 μL/well methanol for 5 min, the cells were stained by 1 times Hoechst 33342 reaction in the dark at room temperature for 30 min. After that, cells were sealed with 100 μL/well anti-fluorescence quenching mounting medium and photographed under a fluorescence microscope. Three random fields were selected to count the number of positive cells under a microscope. EdU labeling rate (%) = the number of positive cells/the number of total cells × 100%.

Scratch Test

A 10-μL of pipette head was used to scratch a horizontal line in the single layer of cells. Next, cells were incubated with serum-free medium for 24 h and observed under an inverted microscope at the 0^{th} and 48^{th} h. The relative distance of cells on both sides of the scratch was measured: relative migration distance = distance difference/2; relative migration rate = relative migration distance/the distance between the edge and median of the scratch at the 0^{th} h.

Transwell Assay

Transwell chamber (aperture, 8 mm; Corning Glass Works, Corning, NY, USA) containing Matrigel was used to assess cell invasion *in vitro*. The basolateral chamber was balanced with 600 mL DMEM containing 20% FBS at 37°C for 1 h. After 48 h of transfection, the cells (1×10^6 cells/mL) were resuspended in FBS-free DMEM and inoculated into the apical chamber for 24 h at 37°C with 5% CO_2. Transwell chambers were fixed by 5% glutaraldehyde at 4°C, stained with 0.1% crystal violet for 5 min, and observed under an inverted fluorescence microscope (TE2000; Nikon, Tokyo, Japan). Five random fields were selected to count the number of cells passing through the chamber.

Dual Luciferase Reporter Assay

The target relationship, as well as the binding sites between CDX2 and miR-181d-5p, was analyzed, based on biological prediction website https://cm.jefferson.edu/rna22/Interactive/, which was verified by

dual luciferase reporter assay. The 3′ UTR region of CDX2 containing miR-181d-5p binding sites (CDX2-WT) and the mutant form in which the binding sites were mutated (CDX2-MUT) were inserted into the luciferase reporter vector. 293T cells were transfected with CDX2-WT or CDX2-MUT, together with miR-181d-5p mimic. 48 h later, the luciferase activity was measured following the manuals of the dual luciferase reporter gene assay kit (D0010; Beijing Solarbio Life Sciences, Beijing, China) by the GloMax 20/20 Luminometer fluorescence detector (Promega, Madison, WI, USA).

ChIP

A ChIP kit (Merck Millipore, Billerica, MA, USA) was utilized to study the enrichment of CDX2 in the HOXA5 gene promoter region. Cells were crosslinked at room temperature for 10 min. After that, an ultrasonic wave was used to fracture DNA. After cells were centrifuged at 4°C, the supernatant was collected, which was, respectively, incubated with positive control antibody RNA polymerase II, NC antibody normal IgG, and target protein-specific rabbit antibody HOXA5 (ab82645; Abcam, Cambridge, MA, USA) at 4°C overnight. Protein agarose/Sepharose was used to precipitate an endogenous DNA-protein compound, which was de-crosslinked at 65°C overnight. Phenol/chloroform was utilized to extract, purify, and recycle DNA fragments. Quantitative real-time PCR was applied to detect the enrichment of the HOXA5 promoter region.

FISH

The expression of miR-181d-5p in tumor stroma and nests was detected by the FISH kit (Roche, Basel, Switzerland). Digoxin-labeled pan-CK and α-SMA probes, as well as the miR-181d-5p probe, were purchased from Sigma-Aldrich (St. Louis, MO, USA). The fluorescence images were captured using the laser confocal scanning microscope (FV1000; Olympus, Tokyo, Japan).

Xenograft Tumor in Nude Mice

Thirty female BALB/c mice (aged 3–5 weeks, weighing 15–20 g; Shanghai Experimental Animal Center of Chinese Academy of Science) were fed in a specific pathogen-free (SPF)-grade clean layer with a barrier system at 24–26°C and the relative humidity of 40%–60%. Ultraviolet radiation was conducted indoors at regular intervals, and the cage, padding, drinking water, and fodder were all sterilized under high pressure. Next, MCF-7 cell suspension was adjusted into 1×10^6 cells/mL by PBS, 50 μL of which was subcutaneously injected into the right side of mice. After 1 week, 24 successfully modeled mice were treated with exo-mimic NC, exo-miR-181d-5p mimic, exo-inhibitor NC, or exo-miR-181d-5p inhibitor by tail-vein injection (six mice each group), 5 days a week. After 36 days, the mice were euthanized by pentobarbital sodium (100 mg/kg, P3761; Sigma-Aldrich, St. Louis, MO, USA), and the tumor was isolated. A ruler was used to record the minor axis (a) and major axis (b) of the tumor, and tumor volume was calculated according to the formula $\pi(a2b)/6$. The tumor weight was measured by a scale. At last, the tumor tissues of nude mice were fixed by 10% formaldehyde, dehydrated, embedded in paraffin, and sectioned into 4 μm of slices.

Statistical Analysis

All data were preceded using SPSS 21.0 software (IBM, Armonk, NY, USA). If the data were consistent with normal distribution and homogeneity of variance, then the measurement data were presented as the mean ± SD. Comparisons between two groups were analyzed by independent t test, comparisons within groups were analyzed by paired t test, comparisons among multiple groups were analyzed using one-way ANOVA with Dunnett's post hoc test, and comparisons of data at various time points were analyzed by repeated-measurement ANOVA with Dunnett's post hoc test. A value of $p < 0.05$ was considered statistically significant.

AUTHOR CONTRIBUTIONS

H. Wang and H. Wei designed the study. J.W. and L.L. collated the data, carried out data analyses, and produced the initial draft of the manuscript. H. Wang, H. Wei, A. Chen, and Z.L. contributed to drafting the manuscript. All authors have read and approved the final submitted manuscript.

CONFLICTS OF INTEREST

The authors declare no competing interests.

ACKNOWLEDGMENTS

We give our sincere gratitude to the reviewers for their valuable suggestions. This study was supported by the National Natural Science Foundation of China (no. 81573001) and the National Natural Science Foundation (81872157) to H. Wang and the Harbin Applied Technology Research and Development Project Plan (Harbin Science and Technology Bureau) (no. 2016RAQXJ174).

REFERENCES

1. Harbeck, N., and Gnant, M. (2017). Breast cancer. Lancet *389*, 1134–1150.
2. Lee, S.Y., and Seo, J.H. (2018). Current Strategies of Endocrine Therapy in Elderly Patients with Breast Cancer. BioMed Res. Int. *2018*, 6074808.
3. Huillard, O., Le Strat, Y., Dubertret, C., Goldwasser, F., and Mallet, J. (2019). RE: Associations Between Breast Cancer Survivorship and Adverse Mental Health Outcomes: A Systematic Review. J. Natl. Cancer Inst. *111*, 335–336.
4. Erdogan, B., and Webb, D.J. (2017). Cancer-associated fibroblasts modulate growth factor signaling and extracellular matrix remodeling to regulate tumor metastasis. Biochem. Soc. Trans. *45*, 229–236.
5. Soon, P.S., Kim, E., Pon, C.K., Gill, A.J., Moore, K., Spillane, A.J., Benn, D.E., and Baxter, R.C. (2013). Breast cancer-associated fibroblasts induce epithelial-to-mesenchymal transition in breast cancer cells. Endocr. Relat. Cancer *20*, 1–12.
6. Huang, X., Yuan, T., Tschannen, M., Sun, Z., Jacob, H., Du, M., Liang, M., Dittmar, R.L., Liu, Y., Liang, M., et al. (2013). Characterization of human plasma-derived exosomal RNAs by deep sequencing. BMC Genomics *14*, 319.
7. Thind, A., and Wilson, C. (2016). Exosomal miRNAs as cancer biomarkers and therapeutic targets. J. Extracell. Vesicles *5*, 31292.
8. Yang, F., Ning, Z., Ma, L., Liu, W., Shao, C., Shu, Y., and Shen, H. (2017). Exosomal miRNAs and miRNA dysregulation in cancer-associated fibroblasts. Mol. Cancer *16*, 148.
9. Donnarumma, E., Fiore, D., Nappa, M., Roscigno, G., Adamo, A., Iaboni, M., Russo, V., Affinito, A., Puoti, I., Quintavalle, C., et al. (2017). Cancer-associated fibroblasts release exosomal microRNAs that dictate an aggressive phenotype in breast cancer. Oncotarget *8*, 19592–19608.
10. Strotbek, M., Schmid, S., Sánchez-González, I., Boerries, M., Busch, H., and Olayioye, M.A. (2017). miR-181 elevates Akt signaling by co-targeting PHLPP2 and INPP4B phosphatases in luminal breast cancer. Int. J. Cancer *140*, 2310–2320.

11. Chen, H., Xiao, Z., Yu, R., Wang, Y., Xu, R., and Zhu, X. (2018). miR-181d-5p-FOXP1 feedback loop modulates the progression of osteosarcoma. Biochem. Biophys. Res. Commun. *503*, 1434–1441.

12. Saito, M., Okayama, H., Saito, K., Ando, J., Kumamoto, K., Nakamura, I., Ohki, S., Ishi, Y., and Takenoshita, S. (2017). CDX2 is involved in microRNA-associated inflammatory carcinogenesis in gastric cancer. Oncol. Lett. *14*, 6184–6190.

13. Yap, C.S., Sinha, R.A., Ota, S., Katsuki, M., and Yen, P.M. (2013). Thyroid hormone negatively regulates CDX2 and SOAT2 mRNA expression via induction of miRNA-181d in hepatic cells. Biochem. Biophys. Res. Commun. *440*, 635–639.

14. Zhou, Z.C., Wang, J., Cai, Z.H., Zhang, Q.H., Cai, Z.X., and Wu, J.H. (2013). Association between vitamin D receptor gene Cdx2 polymorphism and breast cancer susceptibility. Tumour Biol. *34*, 3437–3441.

15. Wang, C.C., Su, K.Y., Chen, H.Y., Chang, S.Y., Shen, C.F., Hsieh, C.H., Hong, Q.S., Chiang, C.C., Chang, G.C., Yu, S.L., and Chen, J.J. (2015). HOXA5 inhibits metastasis via regulating cytoskeletal remodelling and associates with prolonged survival in non-small-cell lung carcinoma. PLoS ONE *10*, e0124191.

16. Jeannotte, L., Gotti, F., and Landry-Truchon, K. (2016). Hoxa5: A Key Player in Development and Disease. J. Dev. Biol. *4*, 13.

17. Teo, W.W., Merino, V.F., Cho, S., Korangath, P., Liang, X., Wu, R.C., Neumann, N.M., Ewald, A.J., and Sukumar, S. (2016). HOXA5 determines cell fate transition and impedes tumor initiation and progression in breast cancer through regulation of E-cadherin and CD24. Oncogene *35*, 5539–5551.

18. Lacle, M.M., van Diest, P.J., Goldschmeding, R., van der Wall, E., and Nguyen, T.Q. (2015). Expression of connective tissue growth factor in male breast cancer: clinicopathologic correlations and prognostic value. PLoS ONE *10*, e0118957.

19. Woolston, C. (2015). Breast cancer. Nature *527*, S101.

20. Luo, H., Tu, G., Liu, Z., and Liu, M. (2015). Cancer-associated fibroblasts: a multifaceted driver of breast cancer progression. Cancer Lett. *361*, 155–163.

21. Taylor, M.A., Sossey-Alaoui, K., Thompson, C.L., Danielpour, D., and Schiemann, W.P. (2013). TGF-β upregulates miR-181a expression to promote breast cancer metastasis. J. Clin. Invest. *123*, 150–163.

22. Shah, S.S., Wu, T.T., Torbenson, M.S., and Chandan, V.S. (2017). Aberrant CDX2 expression in hepatocellular carcinomas: an important diagnostic pitfall. Hum. Pathol. *64*, 13–18.

23. Neumann, J., Heinemann, V., Engel, J., Kirchner, T., and Stintzing, S. (2018). The prognostic impact of CDX2 correlates with the underlying mismatch repair status and BRAF mutational status but not with distant metastasis in colorectal cancer. Virchows Arch. *473*, 199–207.

24. Feng, F., Ren, Q., Wu, S., Saeed, M., and Sun, C. (2017). Hoxa5 increases mitochondrial apoptosis by inhibiting Akt/mTORC1/S6K1 pathway in mice white adipocytes. Oncotarget *8*, 95332–95345.

25. Henderson, G.S., van Diest, P.J., Burger, H., Russo, J., and Raman, V. (2006). Expression pattern of a homeotic gene, HOXA5, in normal breast and in breast tumors. Cell. Oncol. *28*, 305–313.

26. Tabariès, S., Lapointe, J., Besch, T., Carter, M., Woollard, J., Tuggle, C.K., and Jeannotte, L. (2005). Cdx protein interaction with Hoxa5 regulatory sequences contributes to Hoxa5 regional expression along the axial skeleton. Mol. Cell. Biol. *25*, 1389–1401.

27. Liu, P.F., Kang, B.H., Wu, Y.M., Sun, J.H., Yen, L.M., Fu, T.Y., Lin, Y.C., Liou, H.H., Lin, Y.S., Sie, H.C., et al. (2017). Vimentin is a potential prognostic factor for tongue squamous cell carcinoma among five epithelial-mesenchymal transition-related proteins. PLoS ONE *12*, e0178581.

28. Sullivan, N.J., Sasser, A.K., Axel, A.E., Vesuna, F., Raman, V., Ramirez, N., Oberyszyn, T.M., and Hall, B.M. (2009). Interleukin-6 induces an epithelial-mesenchymal transition phenotype in human breast cancer cells. Oncogene *28*, 2940–2947.

29. Sinh, N.D., Endo, K., Miyazawa, K., and Saitoh, M. (2017). Ets1 and ESE1 reciprocally regulate expression of ZEB1/ZEB2, dependent on ERK1/2 activity, in breast cancer cells. Cancer Sci. *108*, 952–960.

30. Stasinopoulos, I.A., Mironchik, Y., Raman, A., Wildes, F., Winnard, P., Jr., and Raman, V. (2005). HOXA5-twist interaction alters p53 homeostasis in breast cancer cells. J. Biol. Chem. *280*, 2294–2299.

31. Chen, H., Chung, S., and Sukumar, S. (2004). HOXA5-induced apoptosis in breast cancer cells is mediated by caspases 2 and 8. Mol. Cell. Biol. *24*, 924–935.

32. Wu, L., Zhang, X., Zhang, B., Shi, H., Yuan, X., Sun, Y., Pan, Z., Qian, H., and Xu, W. (2016). Exosomes derived from gastric cancer cells activate NF-κB pathway in macrophages to promote cancer progression. Tumour Biol. *37*, 12169–12180.

33. He, Y., Deng, F., Yang, S., Wang, D., Chen, X., Zhong, S., Zhao, J., and Tang, J. (2018). Exosomal microRNA: a novel biomarker for breast cancer. Biomarkers Med. *12*, 177–188.

34. Baroni, S., Romero-Cordoba, S., Plantamura, I., Dugo, M., D'Ippolito, E., Cataldo, A., Cosentino, G., Angeloni, V., Rossini, A., Daidone, M.G., and Iorio, M.V. (2016). Exosome-mediated delivery of miR-9 induces cancer-associated fibroblast-like properties in human breast fibroblasts. Cell Death Dis. *7*, e2312.

35. Eichelser, C., Stückrath, I., Müller, V., Milde-Langosch, K., Wikman, H., Pantel, K., and Schwarzenbach, H. (2014). Increased serum levels of circulating exosomal microRNA-373 in receptor-negative breast cancer patients. Oncotarget *5*, 9650–9663.

36. Lebeau, A., Kriegsmann, M., Burandt, E., and Sinn, H.P. (2014). [Invasive breast cancer: the current WHO classification]. Pathologe *35*, 7–17.

37. Kwan, M.L., Haque, R., Lee, V.S., Joanie Chung, W.L., Avila, C.C., Clancy, H.A., Quinn, V.P., and Kushi, L.H. (2012). Validation of AJCC TNM staging for breast tumors diagnosed before 2004 in cancer registries. Cancer Causes Control *23*, 1587–1591.

38. Atkins, D., Reiffen, K.A., Tegtmeier, C.L., Winther, H., Bonato, M.S., and Störkel, S. (2004). Immunohistochemical detection of EGFR in paraffin-embedded tumor tissues: variation in staining intensity due to choice of fixative and storage time of tissue sections. J. Histochem. Cytochem. *52*, 893–901.

39. Ayuk, S.M., Abrahamse, H., and Houreld, N.N. (2016). The role of photobiomodulation on gene expression of cell adhesion molecules in diabetic wounded fibroblasts in vitro. J. Photochem. Photobiol. B *161*, 368–374.